Journal of Electronics Cooling and Thermal Control, 2016, 6, 62-77
Published Online June 2016 in SciRes. http://www.scirp.org/journal/jectc
http://dx.doi.org/10.4236/jectc.2016.62006

Preparation of Composites by Nitro Aluminothermic Processes, over β–SiAlON Matrix in the SiAlON-SiC-Al_2O_3 System

Z. Kovziridze, N. Nizharadze, N. Darakhvelidze, G. Tabatadze, Z. Mestvirishvili, E. Nikoleishvili, M. Mshvildadze

Department of Chemical and Biological Technologies, Georgian Technical University, Tbilisi, Georgia
Email: kowsiri@gtu.ge

Received 31 March 2016; accepted 12 June 2016; published 15 June 2016

Abstract

Goal: The goal of the research is preparation of SiAlON-containing composite through nitro aluminothermic processes, by the methods of reactive sintering and hot compaction. Method: The composite CH-6 was obtained by the method of reactive sintering, with further grinding and hot compression in vacuum furnace at 1600˚C, under 30 MPa pressure and 10 - 12 min standing at the final temperature. Precursor was prepared in a thermostat at 150^{0}C temperature by double compression. Pressure equaled to 20 - 25 MPa. Results: Physical-technical properties of specimens prepared via hot compaction were investigated. Mechanical strength at compression is 1940 MPa; mechanical strength at bending is 490 MPa; elastic module is 199.5 GPa, HV-11.6 GPa. X-Ray diffraction analysis, electron microscopic and X-ray diffraction Microspectral analysis were used to investigate composite microstructure and phase composition. Composite formulation was defined, the main phases of which were: β-SiAlON, corundum and silicium carbide. Conclusion: Composite CH-6 has been selected from the obtained composites, which is characterized by relatively high physical-technical properties: strength, density and hardness. Materials can be used for making high refractory articles, such as jackets to secure thermocouples, furnace bedding, cutting tools for metal and wood treatment, in rocket spatial technology and others.

Keywords

High Refractory Composite, Reactive Sintering, Nitro Aluminothermic Processes, SiAlON, Corundum, Silicium Nitride, Silicium Carbide

How to cite this paper: Kovziridze, Z., Nizharadze, N., Darakhvelidze, N., Tabatadze, G., Mestvirishvili, Z., Nikoleishvili, E. and Mshvildadze, M. (2016) Preparation of Composites by Nitro Aluminothermic Processes, over β–SiAlON Matrix in the SiAlON-SiC-Al_2O_3 System. *Journal of Electronics Cooling and Thermal Control*, **6**, 62-77.
http://dx.doi.org/10.4236/jectc.2016.62006

1. Introduction

In recent years, SiAlON ceramic is intensely used for fabrication of wear resistant, abrasive, construction designation objects since it is characterized by unique mechanical properties, thermal resistance and simultaneously resistance to the impact of chemical medium at high temperatures. This enables us to call SiAlONs "smart super ceramics".

SiAlONs are used in various spheres of technology. Irrespective of a great number of works of researchers of many countries [1]-[9] dedicated to preparation of SiAlONs, methods of SiALONs synthesis offered in those papers, mostly used in laboratory experiments, there is rather scarce information about methods of their industrial preparation. It is connected with high sensitivity of the products of synthesis to chemical composition of raw material and parameters of the processes going on during synthesis which complicate forecasting of phase composition of target products.

With this in view, study of regularities of SiAlON synthesis and selection of reliable methods to receive new functional materials are the urgent task for modern materials science.

SiAlONs are distinguished according to their crystalline structure, silicium nitride, silicium oxynitride, aluminum nitride, mullite structure and diverse Al:Si ratio [10]-[13]. Crystalline structure of SiAlON is similar to the structure of the substance to which the medium of its formation is closer. There are several types of SiAlONs: α; β; X; O^1; H; R. Methods of SiAlON synthesis differ by initial material and conditions of the procedure (temperature, duration, pressure, atmosphere composition). General formula of β-SiALON is: $Si_{6-X}Al_xO_xN_{8-X}$ (where $x = 0 \div 4.2$).

It is considered that SiAlON is a solid solution of Si_3N_4 with aluminum nitride and oxide [14]-[18].

The system Si-Al-O-N can be presented as four-component, schematically given tetrahedron, with the constituting elements at vertexes (**Figure 1**).

Structures and names of SiAlON phases are given in **Table 1** [19]-[21].

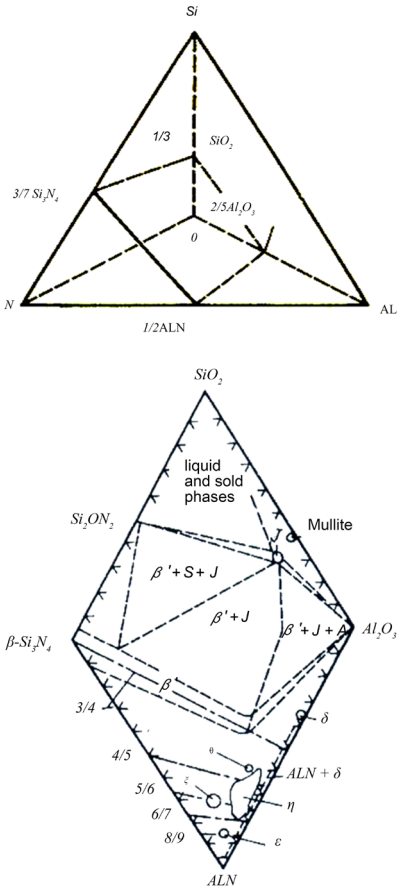

Figure 1. Versions of schemes of distribution of constituting components in Si-Al-O-N system.

Table 1. Names and structures of SiAlON phases.

Name	SiAlON's chemical formula	SiAlON's structure type
α	$Me_x(SiAl)_{12}(ON)_{16}$ X = 0 ÷ 2	α-Si_3N_4
β	$Si_{6-X}Al_xN_{8-X}$ X = 0 ÷ 4.2	β-Si_3N_4
O[1]	$Si_{2-X}Al_X\ O_{1+X}N_{2-X}$ X = 0.04 ÷ 0.4	Si_2ON_2
X	$Si_{2-X}Al_{1-X}O_xN_{1-X}$ X = 0.04 ÷ 0.2	$3Al_2O_3{\cdot}2SiO_2$
H	$SiAl_3O_2N_3$ $SiAl_5O_2N_5$	AAlN
R	$SiAl_4O_2N_4$ $SiAl_6O_2N_6$	AAAlN

2. Major Part

Composites were prepared via the method of reactive sintering and nitro aluminothermic processes by sintering at 1450˚C in nitrogen medium (**Table 2**) [22]-[28].

Initial materials used in the synthesis were: geopolymer, aluminum powder, silicium, silicium carbide, aluminum oxide. To inhibit growth of crystals in the composite and to improve sintering process we used magnesium oxide and oxide of rare earth element–yttrium, as admix. MgO and Y_2O_3 were added to the powder at 1 and 1.5 mass%, correspondingly. High melting temperature of oxides provides for creation of high temperature eutectic melt in the mixture at its heating, which contributes to material sintering process, which is essential for obtaining objects characterized by high thermal resistance and strength.

To improve the sintering process we added glass perlite and refractory clay in small quantities. We compiled mixes and offer their compositions in **Table 2**.

A mix was prepared according to the materials and concentrations given in **Table 2**; specimens were molded into cylinders, with sizes: d—15 mm, h—15 mm, under 20 mPa pressure, by semi-dry method—moisture equaled to 8%. At 110˚C, after drying, specimens were sintered at 1450˚C, under nitrogen medium, with 1 hr standing. A device used for specimen sintering is given in **Figure 2**, while temperature regime for sintering in **Figure 3**.

A device for silicium specimens sintering (**Figure 2**) consists of a furnace (1), silicium carbide heaters, mark TK 30/200. Nitrogen is supplied to the furnace from the bottle (2) through rubber pipe, with a tap on it (3). At the entrance of the furnace velocity of nitrogen coming from the bottle (4) through choke is regulated .Then nitrogen enters refractory corundum pipe (5), which is hermetically closed from both ends. From one end the pipe is supplied with nitrogen and at the exit of the second end, there is a choke with water (6). It regulates pressure in the furnace so that the velocity of nitrogen leaving the pipe was lower than the velocity of nitrogen that enters the reaction pipe. Then nitrogen is released to atmosphere. Furnace temperature is regulated by a transformer (7) and a voltmeter (8) connected to it, while temperature is measured by means of a millivoltmeter (9) and platinum-rhodium thermocouple (10). Rate of increase of temperature is 250˚C/hour. Pressure in nitrogen bottle is regulated by a reducer, which is fixed at the nitrogen bottle.

Physical-technical properties of the obtained specimens have been investigated and are given in **Table 3**.

To receive the material to be characterized with high exploitation properties we selected the composite CH-6. Specimens sintered at 1450˚C were ground and prepared for hot compaction. Precursor was prepared in a thermostat at 150˚C and was cold pressed twice at 15 and 25 mPa; it was hot pressed at 1600˚C under 30 mPa, Vacuum equaled to 10^{-3} Pa, standing at final temperature–10 - 12 min.; sintering regime was: from 20˚C to 500˚C, 7˚C/min, from 500 to 1400˚C, 5˚C/min, from 1400˚C to 1600˚C, 10˚C/min; cooling 10˚C/min. Temperature regime of sintering is offered on **Figure 4**.

We have investigated physical-technical indices of specimens hot-compacted at 1600˚C. The results are offered in **Table 4**. Open porosity of hot-compacted specimens equals to 0.5%, while limit of strength at compaction—1940 MPa; hardness—1140. Considering the data given in the Table we can conclude that 1600˚C is sufficient for complete hardening of specimens.

Table 5 offers micromechanical characteristics of hot-compacted specimens.

Figure 2. A device designed for sintering via nitro aluminothermic processes created by us at the Bio-nanoceramic and Nanocomposite Materials Science Center of Georgian Technical University.

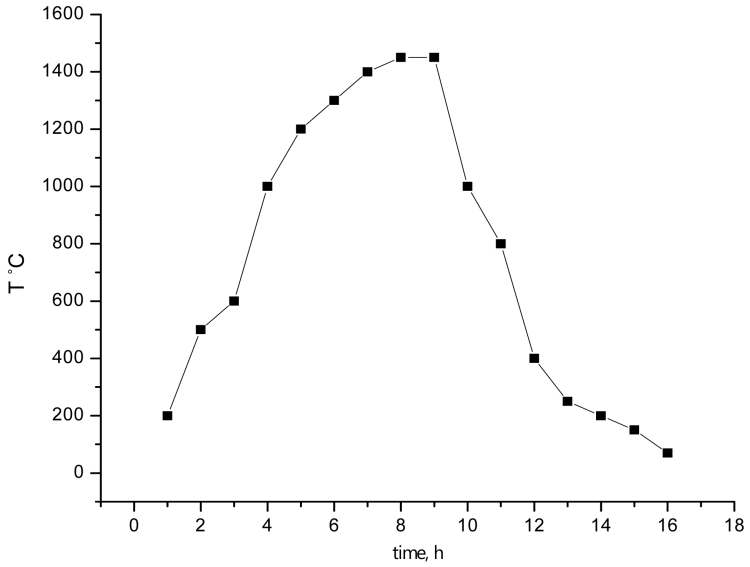

Figure 3. Temperature regime for sintering of the obtained specimens by the method of reactive sintering.

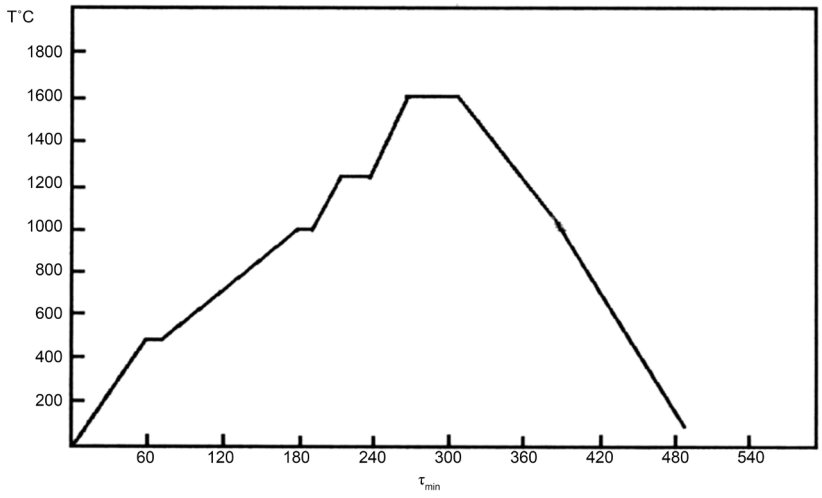

Figure 4. Temperature module for sintering of hot-compacted specimens.

Table 2. Composition of mixes.

Concentration of starting components, mass.%									
Composite index	Kaolin, of Prosianaya (Ukraine)	Al	Al_2O_3	SiC	Si	Perlite of Aragats (Armenia)	Y_2O_3	MgO	Clay of Polog (Ukraine)
CH-6	**15**	**20**	**20**	**20**	**22**	**3**	**2**	**1**	**5**
CH-7	**15**	**25-30**	**27**	**3**	**2**	**1**	**5**		
CH-8	**15**	**25**	**30-27**	**3**	**2**	**1**	**5**		

Table 3. Properties of the composites obtained by reactive sintering.

Composite index	Open porosity w, %	Ultimate strength at compaction, MPa	Density, ρ, g/cm^3	Chemical resistance, %	
				water	acid
CH-6	**15.2**	**256**	**2.25**	**99.82**	**99.20**
CH-7	**15.2**	**258**	**2.31**	**99.79**	**99.25**
CH-8	**15.4**	**254**	**2.78**	**99.80**	**99.30**

Table 4. Physical-technical indices of hot-compacted CH-6 specimen.

Composite index	Open porosity w, %	General porosity $\prod$, %	Density, ρ, g/sm^3	Pressure, during compact. MPa	Ultimate strength at compaction MPa	Ultimate strength at bending MPa
CH-6 (1600^0)	0.5	3.95	2.97	30	1940	490

Table 5. Micromechanical characteristics of hot-compacted specimen CH-6.

Composite index	Kic, Nmm$^{3/2}$	Brittleness factor , B, 1/μm$^{1/2}$	n-factor	HV, GPa.
CH-6 (1600^0)	4.6	2.4	−0.75	11.60

Lawn and Marshall [29] [30] have also introduced quantitative brittleness factor (B), which can be obtained experimentally by dividing micro hardness value by the critical stress intensity factor (Kic) of the specimen: B = Hv/Kic. A lower brittleness factor means lower probability of catastrophic crack propagation in a specimen during machining.

$$\mathrm{Kic} = 0.035 \cdot Hv\sqrt{a} \Big/ \Phi\left(\mathrm{Hv}/\Phi\mathrm{E}\right)^{2/5} \sqrt{1/a}\ \mathrm{Nmm}^{3/2}$$

where Φ: form factor; l: crack length; a: averaged half of impression diagonal; E: elasticity module.

For machining of materials n-factor is an important parameter [31]. This factor enables us to speak about easiness of its machining; n = 0.643 - 0.122 HV. It is claimed that a specimen can be easily machined if it has a positive n value and cannot be easily machined if it has a negative n. In case of our material, treatment by cutting as well as machining for grinding is difficult due to high hardness of the material. We have to state that in the process of disk cutting by diamond disk we came across with high resistance, which damaged some diamond saws and it, quite naturally resulted in propagation of cracks in the material. This reduced mechanical properties of the material to a certain degree. It would be better to have the possibility to perform laser cutting treatment. Dynamic microhardness and elasticity modules were determined on dynamic ultra microhardness tester DUH-211S corresponding to the demands of ISO-14577 International Standards, which is generally used for determination of mechanical characteristics of solid bodies surfaces. Results are offered in **Table 6** and **Table 7**.

Table 6 offers results of tests performed on the specimen CH-6 hot-compacted at 1600˚C. Impressions are taken in matrix. Impressions were taken several times, and results are given in the Table, where average hardness HV: 11.60 GPa.

Dynamic microhardness (DH) was determined in the process of testing according to the load force value on the

Table 6. Test condition-CH6-1600(200gr.).

Test mode	Load-unload		
Sample name	CH6-1600	Sample No.	CH6-1600#1
Test force	200. [gr]	Minimum force	1.96 [mN]
Loading speed	1.0 (70.0670 [mN/sec])	Hold time at load	5 [sec]
Hold time at unload	3 [sec]	Test count	9
Parameter name		Parameter	20
Comment	20.11.15. CH6-1600-matrix		
Poisson's ratio	0.250		
		Indenter type	Vickers
Read times	2	Objective lens	50

Indenter elastic 1.140e+006 [N/mm2] Indenter Poisson's ratio 0.070.

Test result

SEQ	Fmax [mN]	hmax [um]	hp [um]	DHV-1	DHV-2	Eit [N/mm^2]	Length [um]	HV	Data name
1	1908.95	3.0142	1.7431	1047.406	3131.972	2.091e+005	17.398	1192.648	CH6-1600(1900)(1)
2	1908.23	3.0219	1.7539	1041.627	3092.396	2.005e+005	17.693	1152.726	CH6-1600(1900)(4)
3	1907.52	3.0035	1.7088	1054.060	3256.384	2.013e+005	16.816	1275.658	CH6-1600(1900)(7)
4	1908.23	3.1456	1.8419	961.333	2803.722	1.917e+005	18.936	1006.299	CH6-1600(1900)(8)
5	1908.95	3.0214	1.7364	1042.405	3155.932	1.950e+005	18.349	1072.153	CH6-1600(1900)(9)
Average	1908.38	3.0413	1.7568	1029.366	3088.081	1.995e+005	17.838	1140.897	
Std. Dev.	0.601	0.059	0.050	38.354	170.099	6645.808	0.826	104.661	
CV	0.032	1.932	2.869	3.726	5.508	3.331	4.630	9.182	

Table 7. Test condition-CH6-1600(100 gr).

Test mode	Load-unload		
Sample name	CH6-1600	Sample No.	CH6-1600#1
Test force	100 [gr]	Minimum force	1.96 [mN]
Loading speed	1.0 (70.0670 [mN/sec])	Hold time at load	5 [sec]
Hold time at unload	3 [sec]	Test count	7
Parameter name		Parameter	20
Comment	20.11.15. SH6-1600-(Matrix)		
Poisson's ratio	0.250		
Cf-Ap,As Correction	ON	Indenter type	Vickers
Read times	2	Objective lens	50

Indenter elastic 1.140e+006 [N/mm^2] Indenter Poisson's ratio 0.070.

Test result

SEQ	Fmax [mN]	hmax [um]	hp [um]	DHV-1	DHV-2	Eit [N/mm^2]	Length [um]	HV	Data name
1	1006.17	2.1999	1.2690	1036.372	3114.721	2.004e+005	13.159	1098.818	CH6-1600(1000)(1)
2	1010.12	2.2287	1.2636	1013.712	3153.815	1.938e+005	12.428	1236.728	CH6-1600(1000)(2)
3	1005.82	2.1582	1.2364	1076.444	3280.092	2.134e+005	12.866	1149.012	CH6-1600(1000)(3)
4	1007.07	2.1779	1.2338	1058.338	3297.626	2.075e+005	13.084	1112.414	CH6-1600(1000)(5)
5	1006.89	2.1948	1.2499	1041.979	3212.885	1.998e+005	12.719	1177.018	CH6-1600(1000)(7)
Average	1007.22	2.1919	1.2505	1045.369	3211.828	2.030e+005	12.851	1154.798	
Std. Dev.	1.704	0.026	0.016	23.603	78.768	7581.317	0.294	55.159	
CV	0.169	1.198	1.258	2.258	2.452	3.735	2.288	4.776	

indenter and depth of its penetration into material; its value was computed by the formula: DH=a x F/h^2; where a is a constant value and depends on indenter form; for Vickers indenter a = 3.8584.

Advantage of the method compared to the common, static method, that is measuring linear sizes of impression (diagonal) is that it consists of both plastic and elastic components. Results of measurements don't depend on impression sizes, load and non-homogeneity of flexibility recovery.

Dynamic hardness was determined in loading-unloading regime, by taking seven readings at each concrete loading, by discarding two end values and by averaging the remaining five values. Corresponding value of micro hardness was determined automatically. Hold-time at maximum load equaled to 5 sec., at the end of unloading 3 sec (**Figure 5(a)** and **Figure 5(b)**) and (**Figure 6(a)** and **Figure 6(b)**).

Indenting was performed in specimen matrix, which consisted of β-SiAlON. Testing has shown that its mean dynamic hardness equals to DHV = 10.29 GPa, which is a rather high value [32]-[34].

From the load-unload ratio graph (**Figure 5**) the elasticity module value is determined by defining rigidity S = (dF/dh) $h\text{-}h_{max}$. It is a tangent of load-unload graph at the starting point of unloading. A device defined flexibility module of the material under the study, which in case of our specimen equals to: E = 199 GPa.

Table 7 offers results of tests performed on the specimen CH-6 hot-pressed at 1600˚C. Impressions are taken in matrix. Impressions were taken several times, and results are given in the Table, where average hardness HV: 11.54 GPa. Elasticity module E = 203 GPa.

Figure 7 shows impression taken in SiAlON matrix, which shows that impression form is clear, with clearly cut edges. Along the edges similar size cracks can be observed which speaks about matrix homogeneity.

Table 8 offers results of testing of SiC grains of the composite CH6-1600 microstructure. Indenting was performed at 199 gr load on grains. Average hardness value HV for silicium carbide was 22.6 gPa; dynamic hardness DH-15.2 GPa, elasticity module E-289 GPa, which are rather high values.

Table 8. Test condition-CH6-1600-(SiC).

Test mode	Load-unload		
Sample name	CH6-1600	Sample No.	CH6-1600
Test force	100 [gr]	Minimum force	1.96 [mN]
Loading speed	1.0 (70.0670 [mN/sec])	Hold time at load	5 [sec]
Hold time at unload	3 [sec]	Test count	5
Parameter name		Parameter	20
Comment	20.11.15. CH6-1600-(SiC)		
Poisson's ratio	0.190		
Cf-Ap,As Correction	ON	Indenter type	Vickers
Read times	2	Objective lens	50

Indenter elastic 1.140e+006 [N/mm^2] Indenter Poisson's ratio 0.070.

Test result

SEQ	Fmax [mN]	hmax [um]	hp [um]	DHV-1	DHV-2	Eit [N/mm^2]	Length [um]	HV	Data name
1	1007.08	2.0103	1.0236	1242.166	4791.258	2.480e+005	10.162	1844.218	CH6-1600(SiC)1(1)
2	1006.75	1.6322	0.7303	1883.813	9404.742	3.630e+005	8.406	2694.000	CH6-1600(SiC)1(2)
3	1006.72	2.0353	0.9926	1211.497	5093.065	2.109e+005	9.577	2075.808	CH6-1600(SiC)1(3)
4	1007.82	1.7741	0.7956	1596.132	7937.545	2.939e+005	9.575	2078.698	CH6-1600(SiC)1(4)
5	1008.72	1.7322	0.8749	1675.821	6569.192	3.307e+005	8.553	2607.470	CH6-1600(SiC)1(5)
Average	1007.42	1.8368	0.8834	1521.886	6759.161	2.893e+005	9.255	2260.039	
Std. Dev.	0.850	0.178	0.125	289.303	1941.153	61304.285	0.749	370.393	
CV	0.084	9.672	14.185	19.009	28.719	21.191	8.088	16.389	

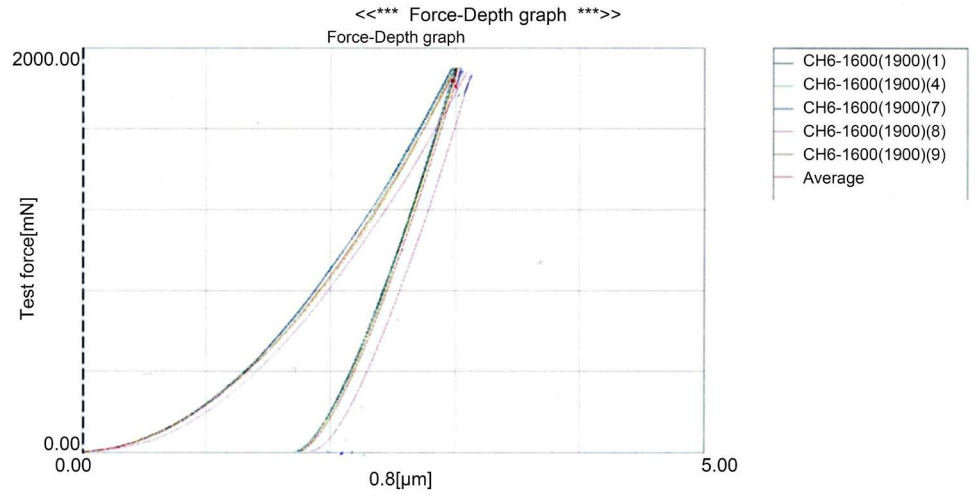
<<*** Force-Depth graph ***>>
Force-Depth graph
2000.00
0.00
Test force[mN]
0.00
0.8[µm]
5.00
CH6-1600(1900)(1)
CH6-1600(1900)(4)
CH6-1600(1900)(7)
CH6-1600(1900)(8)
CH6-1600(1900)(9)
Average

(a)

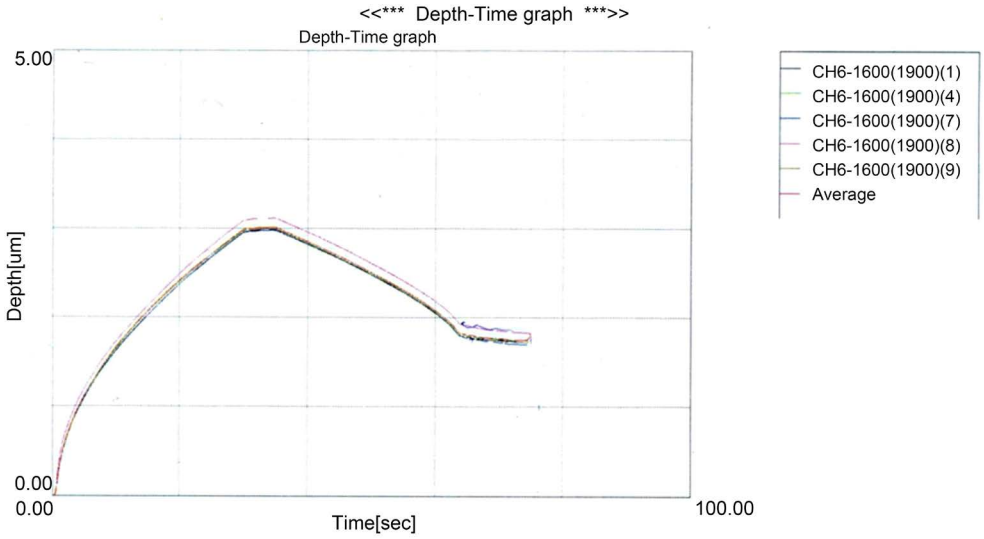
<<*** Depth-Time graph ***>>
Depth-Time graph
5.00
0.00
Depth[um]
0.00
Time[sec]
100.00
CH6-1600(1900)(1)
CH6-1600(1900)(4)
CH6-1600(1900)(7)
CH6-1600(1900)(8)
CH6-1600(1900)(9)
Average

(b)

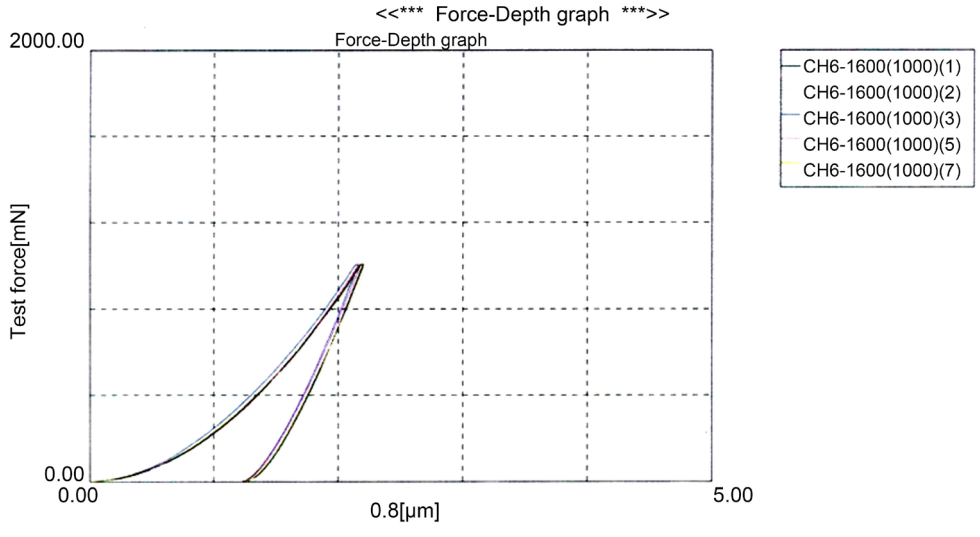
<<*** Force-Depth graph ***>>
Force-Depth graph
2000.00
0.00
Test force[mN]
0.00
0.8[µm]
5.00
CH6-1600(1000)(1)
CH6-1600(1000)(2)
CH6-1600(1000)(3)
CH6-1600(1000)(5)
CH6-1600(1000)(7)

(c)

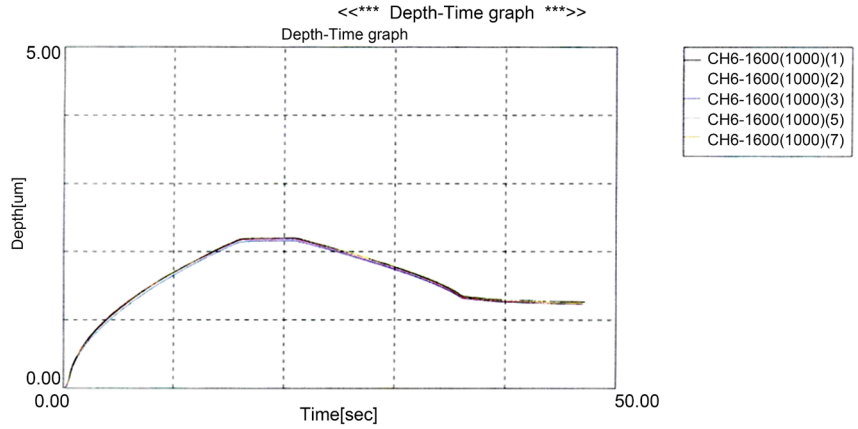

(d)

Figure 5. Load-unload curves: (a), (c) for load force at indenter; (b), (d) depth of indenter penetration into material.

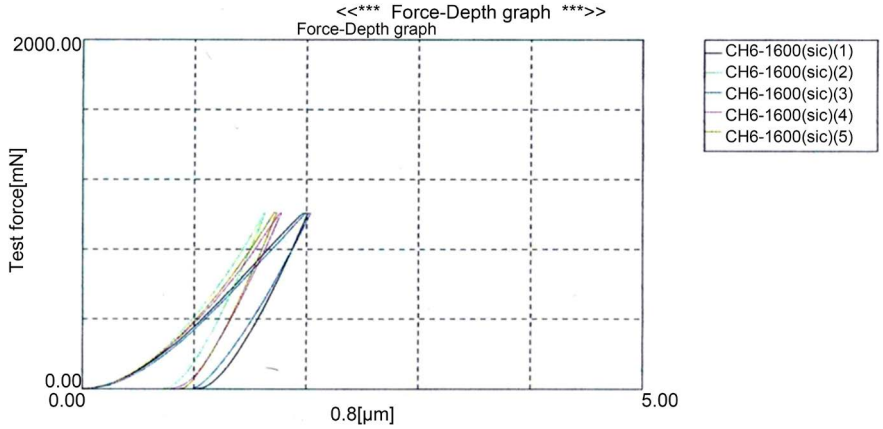

(a)

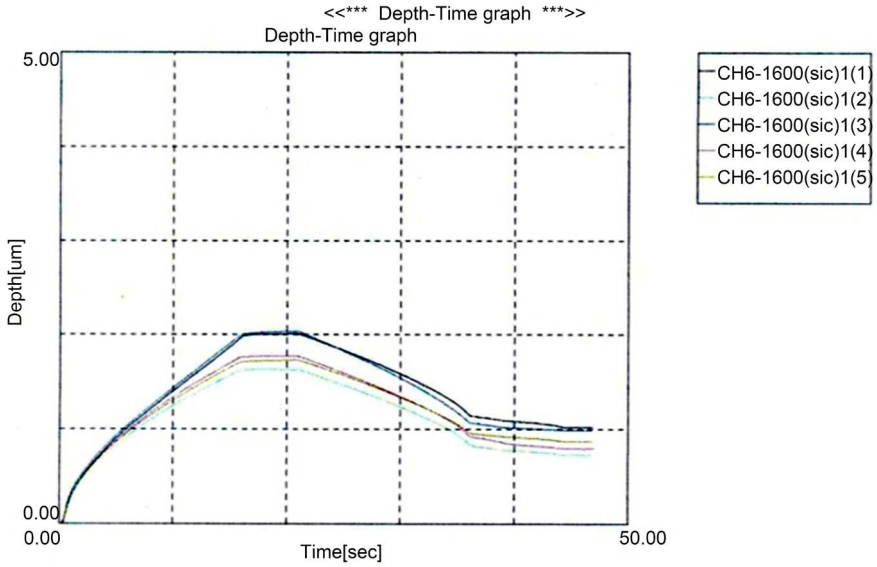

(b)

Figure 6. Load-inload curves for indenter penetration depth into material: (a) load force at indenter; (b) depth of indenter penetration into material.

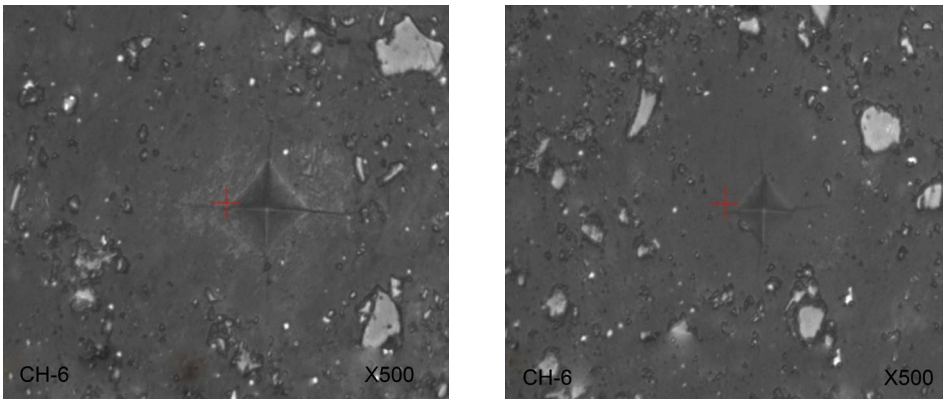

(a) (b)

Figure 7. Impression taken in SiAlON matrix, load (a) 200 gr; (b) 100 gr.

Limits of impressions taken from carbide grains are clear (**Figure 8**); crack, which was created on the grain as a result of indenter load doesn't spread beyond the grain limits, matrix inhibits crack spreading and the composite hardness retains its value.

To investigate phase composition of a composite CH-6 obtained via sintering and hot-compaction at 1600˚C we used X-ray and electron microscopy methods.

X-ray analysis was performed on X-ray diffraction apparatus "DRON-3", roentgenogram was taken at 22.5˚ - 65˚ angle interval, at 2˚ min speed. Both roentgenograms are given in **Figure 9** and **Figure 10**.

Composite X-ray shows diffraction maximums characteristic to SiAlON d_{hkl}: 7.95; 5.63; 3.85; 3.65; 2.520; 2.19; silicium carbide- d_{hkl}: 2.63; 2.370; 2.19; 2.014; corundum-d_{hkl}: 3.49; 2.52; 2.36; 2.090.

As is seen from both X-ray the CH-6 composite consists mainly of β-SiAlON, which has hexagonal structure. Alongside with the β-SiAlON it contains silicium carbide and corundum, which are introduced into the mix from the very beginning. In both cases composite matrix is β-SiAlON and it is hardened by corundum and silicium carbide crystals.

Electron-microscopic studies were performed by JEOL firm electron-raster (scanning) microscope. The method is based on reflection of the reflected electrons and secondary ejected electrons.

To carry out phase analysis of the composite by reflected electrons we broke a specimen parallel to the surface. Fracture must be new. Results are given in **Figure 11** at: a) ×270, b) ×1000, c) ×2200, d) ×2700 magnifications.

Figure 11 shows a matrix consisting of β-SiAlON, which confirms the data of X-ray analysis.

Electron microscopy images of CH-6 composite shows the well sintered specimen surface, with clearly observable crystals of the main phases which are in the composites hot-compacted at 1600˚C, in particular as its matrix—SiAlON, SiC and corundum.

Pores are not observed in any specimen. X-ray diffraction analysis data conform to images of electron microscope analysis. It is apparent that at hot-compaction the mineralogical composition of the composite suffers no changes, compared to the specimens obtained by reactive sintering, which becomes more vivid at greater magnification.

X-ray diffraction microanalysis of the same specimen was performed on OXFORD INSTURMENTALS detector X-max, which enabled us to receive general composition of the composite elements. Results of analysis are given in **Figure 12**.

Figure 12 offers X-ray microanalysis at the spectrum 1 section of CH-6 composite obtained by hot-compaction, together with percentage concentration of the constituting elements; it shows that the main component of the composite is SiAlON.

Figure 12 offers percent composition of SiAlON: silicium, aluminum, oxygen and nitrogen. Besides, the element, carbon was fixed there which refers to the presence of SiC. Increased volume of oxygen and presence of aluminum refer to the presence of SiAlON as well as corundum in the composite.

The schemes for element concentrations are offered for relatively short sections spectrum 2, 3, 4, 5 (**Figure 13**) Schemes mirroring elements concentration at relatively short sections spectrum 2, 3, 4, 5 are offered. X-ray microanalysis of the points given on the image gives clear picture of concentration of elements of phases present

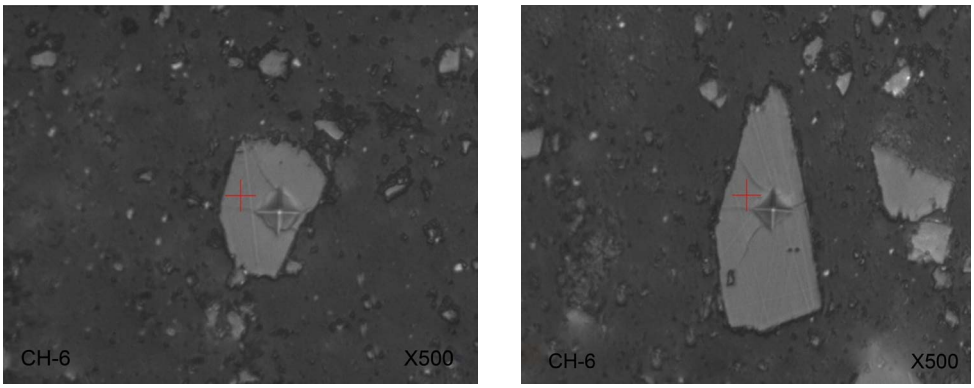

(a) (b)

Figure 8. Impression taken from SiC grain at 100 gr. load.

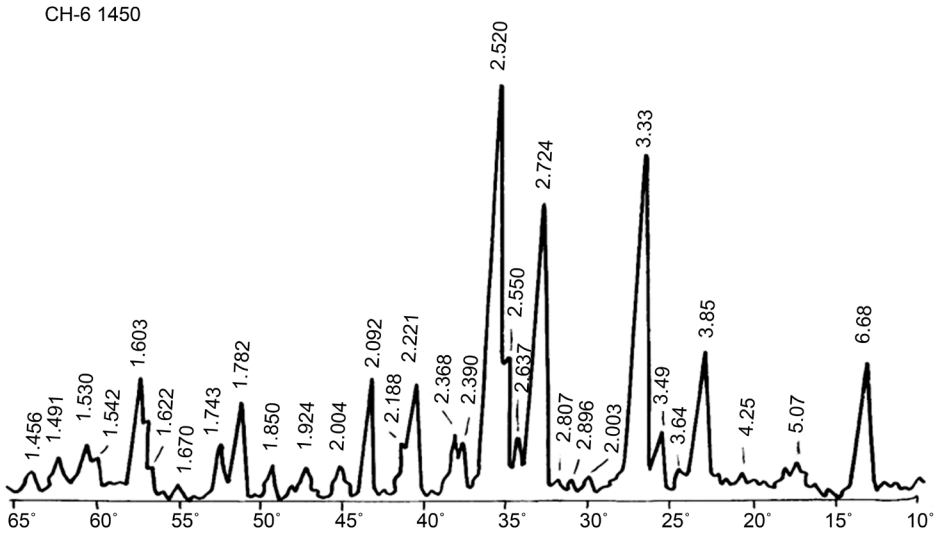

Figure 9. X-ray of CH-6 composite (1450˚).

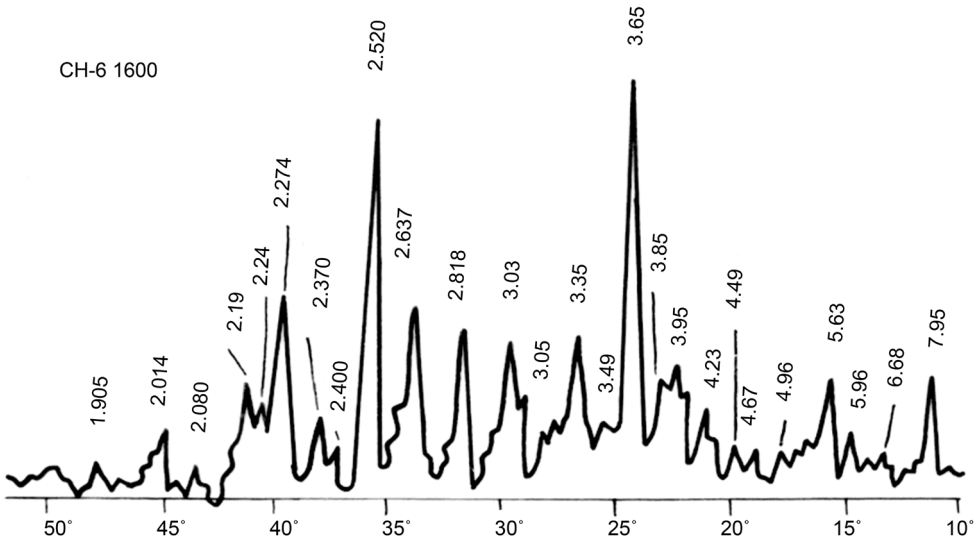

Figure 10. X-ray of CH-6 composite (1600˚).

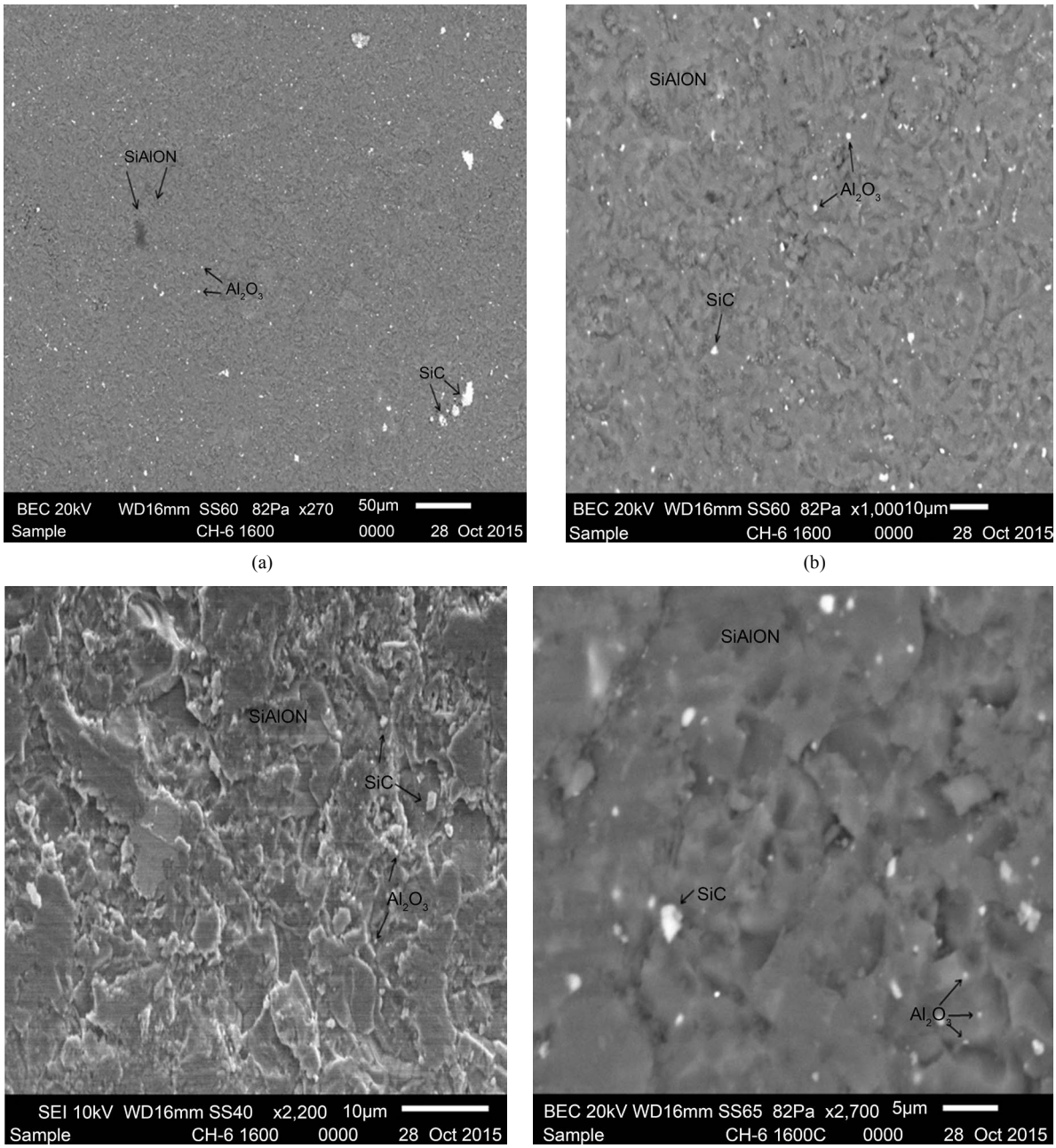

Figure 11. Electron-microscopic images of CH-6 composite at various magnifications: (a) ×270; (b) ×1000; (c) ×2200; (d) ×2700.

namely at those points. The image shows percentage of the constituent elements of the main phases SiAlON, silicium carbide and corundum. At all sections percentage ratio is almost similar, which refers to homogeneous structure of the obtained composite CH-6.

3. Conclusions

CH-6, CH-7 and CH-8 composites were obtained on the base of geopolymer, silicium carbide, aluminum oxide, silicium and aluminum powder by the method of reactive sintering, via nitro aluminothermic processes.

Physical-technical properties and phase composition of the composite were investigated. The main phases are:

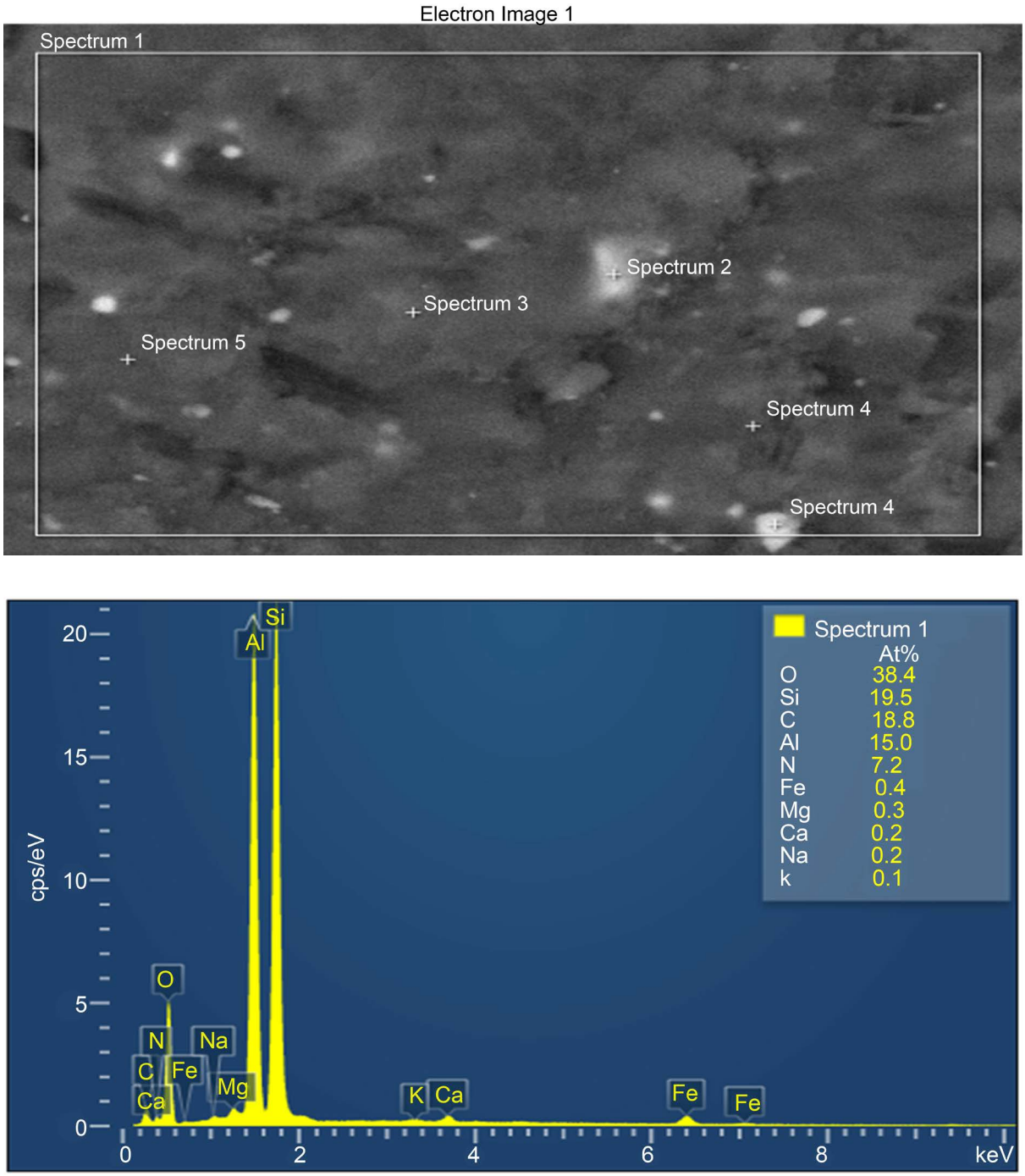

Figure 12. X-ray microanalysis of CH-6 composite in the section spectrum 1.

β-SiAlON, which is a matrix of the composite, silicium carbide and corundum.

The obtained porous (15.2%) composite was regrinded and the precursor was prepared in a thermostat at 150˚C, by double compression at 25 mPa.

Precursor was compacted hotly, in vacuum, at 1600˚C, under 30 mPa and at standing for 10 - 12 min at final temperature. The obtained CH-6 composite is characterized by high hardness HV-11.60, density 2, 97 g/cm^3 and strength at compaction 1940 MPa and strength at bending −490 MPa [35]. Mineralogical composition remained unchanged. Materials, according to their properties can be used for making high refractory articles, such as

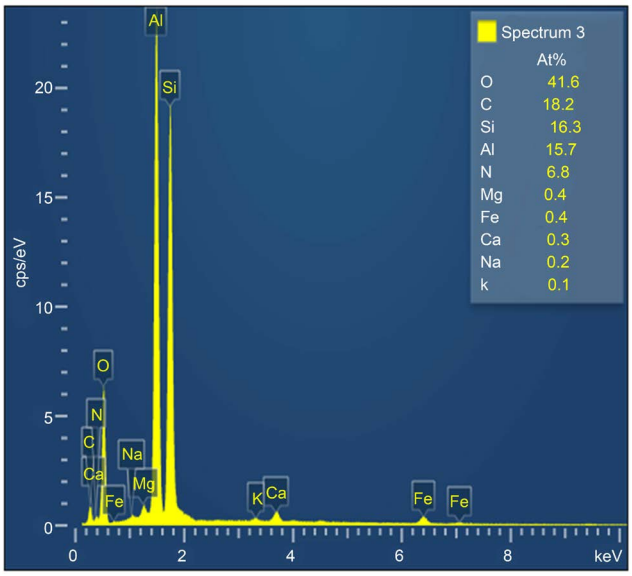
Spectrum 3
At%
O 41.6
C 18.2
Si 16.3
Al 15.7
N 6.8
Mg 0.4
Fe 0.4
Ca 0.3
Na 0.2
k 0.1
cps/eV
keV
Al
Si
O
N
C
Na
Ca
Mg
Fe
K
Ca
Fe
Fe

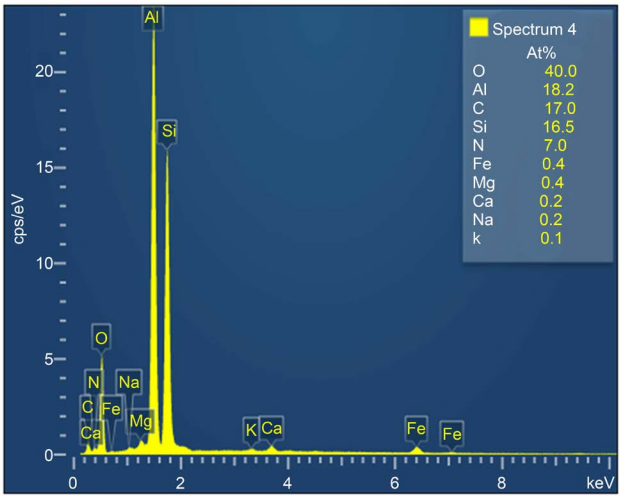
Spectrum 4
At%
O 40.0
Al 18.2
C 17.0
Si 16.5
N 7.0
Fe 0.4
Mg 0.4
Ca 0.2
Na 0.2
k 0.1
cps/eV
keV
Al
Si
O
N
Na
C
Fe
Mg
Ca
K
Ca
Fe
Fe

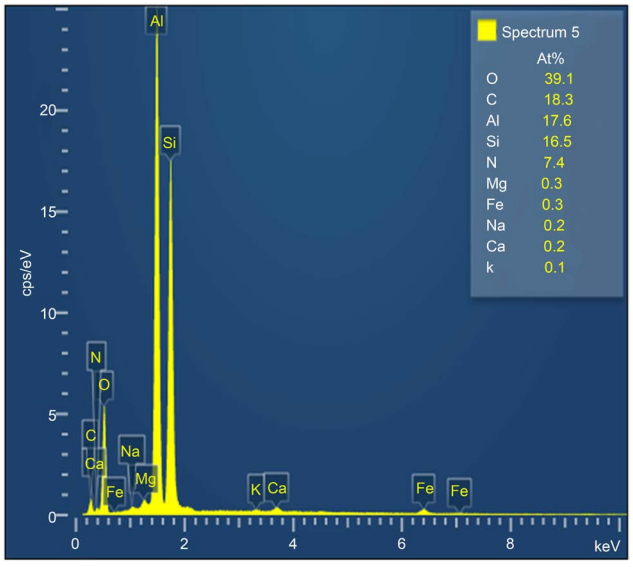
Spectrum 5
At%
O 39.1
C 18.3
Al 17.6
Si 16.5
N 7.4
Mg 0.3
Fe 0.3
Na 0.2
Ca 0.2
k 0.1
cps/eV
keV
Al
Si
N
O
C
Na
Ca
Mg
Fe
K
Ca
Fe
Fe

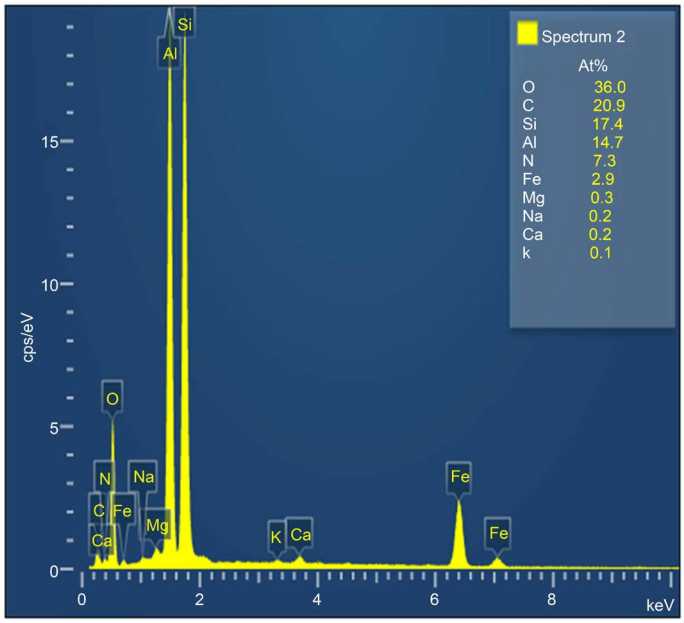

Figure 13. X-ray microanalysis of CH-6 composite in the section 2, 3, 4, 5.

jackets to secure thermocouples, furnace bedding, cutting tools for metal and wood treatment, in rocket spatial technology and others.

References

[1] Zheng, G.M., Zhao, J., Gao, Z.J. and Cao, Q.Y. (2012) Cutting Performance and Wear Mechanisms at Sialon-Si_3N_4 Graded Nano-Composite Ceramic Cutting Tools. *The International Journal of Advanced Manufacturing Technology*, **58**, 19-28.

[2] Belij, Y.U., Komda, V.V., Sivistun, V.M. and Polozhai, S.G. (1990) For the Issue of Preparation of Composite Materials on the Base of Silicium Nitride. *Moscow International Symposium on Composites*, *Abstracts of Reports*, Moscow, November 1990, 174.

[3] Chukholina, L.N. (2012) Method for Obtaining SiAlON Powder. 18 November.

[4] Boyarina, I.L., Puchkov, A.B., *et al.* (1981) SiAlONs, New Refractory Material. *Refractories*, **12**, 24.

[5] Jack, K.H. (1976) Review: Sialons and Related Nitrogen Ceramics. *Journal of Materials Science*, **11**, 1135-1158.

[6] Ekstrom, T. and Persson, J. (1990) Hot Hardness Behavior of Yttrium Sialon Ceramics. *Journal of the American Ceramic Society*, **73**, 2834-2838.

[7] Klemm, H., Herman, M., Reich, T., *et al.* (1998) High Temperature Properties of Mixed *α*/*β*-Sialon Materials. *Journal of the American Ceramic Society*, **81**, 1141-1148.

[8] Washburn, M.E. and Love, R.W. (1962) A Silicon Carbide Refractory with a Complex Nitride Bond Containing Silicon Oxynitride. *American Ceramic Society Bulletin*, **41**, 447-449.

[9] Riley, F.L. (2000) Silicon Nitride and Related Materials. *Journal of the American Ceramic Society*, **83**, 10-30.

[10] Suvorov, S.A., Dolgushev, N.V. and Zaboloysky, A.V. (2002) Thermodynamic Parameters of *β*-SiAlONs. *Inorganic Materials*, **38**, 290-292.

[11] Rosenflanz, A. and Chen, I.W. (1999) Phase Relationships and Stability of Sialon. *Journal of the American Ceramic Society*, **82**, 25-28.

[12] Ekstrom, T., Kall, P.O., Nygren, M. and Olsson, P.O. (1989) Dense Single-Phase Beta-Sialon Ceramics by Glass-Encapsulated Hot Isostatic Pressing. *Journal of Materials Science*, **24**, 1853-1862.

[13] Kovziridze, Z., Nijharadze, N., Tabatadze, G., Cheishvili, T., Mestvirishvili, Z., Nikoleishvili, E., Mshvildadze, M. and Darakhvelidze, N. (2014) Obtaining of Nanocomposites in SiC-SiAlON and Al_2O_3-SiAlON System by Alumothermal Processes. *Journal of Electronics Cooling and Thermal Control*, **4**, 105-115. http://dx.doi.org/10.4236/jectc.2014.44012

[14] Barinov, S.M. and Shevchenko, V.Y. (1993) Technical Ceramics. M., Nauka, p. 187.

[15] Gorshkov, V.S., Saveljev, V.G. and Abakumov, A.V. (1994) Cohesive Material, Ceramics and Glass Crystalline Materials: Structure and Properties: Reference Guide. M., "Stroyizdat", p. 584.

[16] Kishi, K., Umebayashi, S. and Tani, E. (1990) Influence of Microstructure of Strength and Fracture Toughness of *β*-Sialon. *Journal of Materials Science*, **25**, 2780-2784. http://dx.doi.org/10.1007/BF00584879

[17] Piekarczyk, J., Lis, J. and Bialoskorski, J. (1990) Elastic Properties, Hardness and Indentation Fracture Toughness of *β*-Sialons. *Key Engineering Materials*, **89-91**, 541-546.

[18] Jiang, X., Baek, Y.-K., Lee, S.-M. and Kang, S.-J.L. (1998) Formation of an *α*-SiAlON Layer on *β*-SiAlON and Its Effect on Mechanical Properties. *Journal of the American Ceramic Society*, **81**, 1907-1912. http://dx.doi.org/10.1111/j.1151-2916.1998.tb02565.x

[19] Ekström, T. and Nygren, M (1992) SiAlON Ceramics. *Journal of the American Ceramic Society*, **75**, 259-276. http://dx.doi.org/10.1111/j.1151-2916.1992.tb08175.x

[20] Huang, Z.-K., Nunn, S.D., Peterson, I. and Tien, T.-Y. (1994) Formation of N-Phase and Phase Relations in MgO-Si_2N_2O-Al_2O_3 System. *Journal of the American Ceramic Society*, **77**, 3251-3254. http://dx.doi.org/10.1111/j.1151-2916.1994.tb04578.x

[21] Method of Forming a Ceramic Product. Lumby R.J. (GB), 31.05.77. Pat. 4113503 USA, CO4B 035/58.

[22] Kovziridze, Z., Nijaradze, N., Tabatadze, G. and Mestvirishvili, Z. (2014) Carbo- and Alumothermic Processes on the Base of Geopolymer in Nitrogen Medium. *Journal of the Georgian Ceramist's Association*, **1**.

[23] Zalite, I., Zilinska, N. and Kladler, G. (2007) Some Sialons Prepared from Nanopowders by Hot Pressing. *J Journal of Physics Conference Series*, **93**, Article ID: 012008.

[24] Kovziridze, Z., Nijaradze, N., Tabatadze, G., Darakhvelidze, N. and Mestvirishvili, Z. (2015) Application of Alum-Thermal and Nitrogen Methods for Obtaining Nano-Composites in the Systems of SiC-SiAlON and Al_2O_3-SiAlON-Innovative Technologies in Metallurgy and Materials Science. *Georgian Technical University*, *International Conference*, Tbilisi, 16-18 July 2015.

[25] Kovziridze, Z., Nijaradze, N., Tabatadze, G., Darakhvelidze, N. and Mestvirishvili, Z. (2015) Smart Materials in the SiAlON-SiC-Al_2O_3 System. *International Conference and Expo on Ceramics*, Chicago, 17-18 August 2015.

[26] Kovziridze, Z., Nijaradze, N., Tabatadze, G., Cheishvili, T., Darakhvelidze, N., Mestvirishvili, Z., Mshvildadze, M. and Nikoleishvili, E. (2014) Preparation of SiAlONS by Nitro-Alunothermic Processes. *Journal of Georgian Ceramists Association*, **2**, 23-31.

[27] SiAlON-Aluminum-Silicium Oxynitride http://www.ceramtec.com.ua/ceramic-materials/sialon/

[28] Aleksandrov, P.A. and Popova, N.A. (2012) Method for Obtaining Ultra-Dispersive Powder of Beta-SiA-lON. http://www.freepatent.ru/patents/2421428

[29] Lawn, B.R. and Marshall, D.B. (1979) Hardness, Toughness and Brittleness: an Indentation Analysis. *Journal of the American Ceramic Society*, **62**, 347-350. http://dx.doi.org/10.1111/j.1151-2916.1979.tb19075.x

[30] Eftekhari Yekta, B. and Hamnabard, Z. (2013) Investigation of the Mechanical Properties and Machinability of Fluorphlogopite-Gehlenite Glass-Ceramics. *Journal of Ceramic Science and Technology*, **4**, 193-196.

[31] Baik, D.S., No, K.S.,Chun, J. S., Yoon, Y.J. and Cho, H.Y. (1995) A Comparative Evaluation Method of Machinability for Mica-Based Glass-Ceramics. *Journal of Materials Science*, **30**, 1801-1806. http://dx.doi.org/10.1007/BF00351613

[32] Metallic Materials-Instrumented Indentation Test for Hardness and Materials Parameters. BS EN ISO14577-1:2002.

[33] http://www.shimadzu.eu/duh-211duh-211s

[34] Sahin, O., Uzun, O., Sopicka-Lizer, M., Gocmez, H. and Kolemen, U. (2008) Dynamic Hardness and Elastic Modulus Calculation of Porous SiAlON Ceramics Using Depth-Sensing Indentation Technique. *Journal of the European Ceramic Society*, **28**, 1235-1242. http://dx.doi.org/10.1016/j.jeurceramsoc.2007.09.052

[35] Kovziridze, Z., Nijaradze, N., Tabatadze, G., Darakhvelidze, N. and Mestvirishvili, Z. (2016) Smart Materials in the System SiAlON-Sic-Al_2O_3-TiB_2-ZrB_2. *BIT's 2nd Annual World Congress of Smart Materials*, Singapore, 4-6 March 2016, 558.